American Mineralogist, Volume 70, pages 375–378, 1985

Experimental observations on coexisting zoisite–clinozoisite

ARTHUR R. PRUNIER, JR.[1] AND DAVID A. HEWITT

Department of Geological Sciences
Virginia Polytechnic Institute and State University
Blacksburg, Virginia 24061

Abstract

Epitaxial zoisite/clinozoiste crystals hydrothermally synthesized at approximately 650°C and 6500 bar were characterized by X-ray diffraction and electron microprobe techniques to deduce the following thermodynamic relations: $G_{zo} < G_{clz}$ for $X_{Fe} \leq 6$ mole% Ps, and $G_{clz} < G_{zo}$ for $X_{Fe} \geq 19$ mole% Ps (Ps = pistacite molecule). The good correspondence between these values and natural zoisite–clinozoisite pair compositions suggests that single crystal (versus bulk) techniques could be employed to bracket equilibria for phases that are extremely difficult to synthesize with a homogeneous composition.

Introduction

Although coexisting zoisite and clinozoisite have been known for many years (Rodgers, 1924), only recently have the natural occurrences begun to receive detailed examination (Ackermand and Raase, 1973; Enami and Banno, 1980). Experimental investigation of the phase relations of these minerals is also in its infancy. Newton (1965, 1966) and Goldsmith (1981) have determined phase equilibria involving endmember zoisite, and Holdaway (1972), Strens (1965), and Liou (1973) have investigated reactions involving epidote. Only a single recent study (Jenkins et al., 1983) has attempted to outline the stability relations for the zoisite–clinozoisite transition in the iron-free system and no one has experimentally investigated coexisting phases in the iron-bearing system.

The experimental data of Jenkins et al. (1983) and the compositions of coexisting natural zoisite–clinozoisite pairs indicate that the iron-free transition occurs at very low temperatures with zoisite as the high temperature phase. As iron is added, a two-phase transition loop is generated with zoisite as the high-temperature, low-iron phase.

In this paper we present a bracket on the zoisite–clinozoisite transition loop in the iron-bearing system. The data were obtained using new experimental and analytical techniques that do not require the synthesized materials to be compositionally or structurally homogeneous. Because synthetic zoisites and clinozoisites, like their natural counterparts, are highly zoned, classical experimental methods do not yield valid results. By using microanalytical techniques and single crystal X-ray methods on mineral overgrowths, we are able to obtain results consistent with previous experimental and natural data.

Experimental methods

Hydrothermal syntheses of crystalline material were carried out for bulk compositions from pure zoisite ($Ca_2Al_3Si_3O_{12}(OH)$) to a clinozoisite with 16.7 mole% of the pistacite molecule ($Ca_2Al_{2.5}Fe_{0.5}Si_3O_{12}(OH)$). Starting materials for the synthesis runs consisted of stoichiometric mixtures of synthetic anorthite crystallized from a gel, silica glass and certified reagent $CaCO_3$ and Fe_2O_3. Syntheses of zoisite or clinozoisite from these mixes were performed using standard cold-seal hydrothermal techniques with vessels of Rene 41 alloy. Materials were sealed with pure water in either gold or platinum capsules. Runs were conducted at pressures ranging from 5.0 to 6.5 kbar with temperatures in the range of 500 to 650°C. Pressures were measured with a factory-calibrated Heise Bourdon Tube gauge and are believed accurate to ±100 bars. Temperatures were measured with calibrated chromel-alumel thermocouples and are accurate to ±5°C. Synthesis runs typically lasted two to four weeks.

Several "seeded" experients were performed in a similar manner, except that five to ten large zoisite seed crystals (>100 μm) from iron-free synthesis runs were incorporated in the oxide starting material. The resulting overgrowths were then examined as outlined below.

Products were identified using optical and X-ray techniques. Zero-level Weissenberg photographs were found to be necessary to unambiguously identify the selected single crystals of zoisite or clinozoisite. Single crystals so characterized were then analyzed in an ARL-SEMQ electron microprobe. Synthetic anorthite was used as the standard for Ca, Al, and Si, and Marjalati olivine (8.97 wt.% Fe) was used as the Fe standard. Matrix corrections were performed using the ZAF procedure of Springer (1976).

Results

Experimental runs aimed at synthesizing either zoisite or clinozoisite were generally successful (Table 1). However, synthesis runs at the lowest pressure (5.0 kbar) produced mostly garnet and anorthite. Over the limited range of conditions investigated (500 to 650°C and 5.0 to 6.5 kbar), higher temperatures and pressures produced larger crystals. Zoisite and clinozoisite both grew as bladed crystals elon-

[1] Present address: Dow Chemical Corporation, Midland, Michigan.

0003–004X/85/0304–0375$02.00

Table 1. Summary of experimental conditions

	Run No.	Bulk Comp. (mole % Ps)	Temp. (°C)	Pressure (bars)	Run Time (days)	Major Products
Synthesis	42-77	0	500	6500	24	Zo
	12-76	1.7	650		31	Zo
	44-77	3.3	500		29	Zo > Clz
	24-76	10.0	650		33	Zo > Clz
	25-76	11.7	650		33	Clz + Zo overgrowths
	31-76	18.3	650		20	Clz > Zo
	60-77	5.0	650	5800	32	Zo
	62-77	10.0	650		32	Zo > Clz
	33-76	13.3	550		21	Clz > Zo
	63-77	1.7	650	5000	32	Gt + An
	67-77	8.3	650		32	Gt + An
Seeded Runs	105-77	11.7	650	6500	8	Zo + Clz overgrowths
	106-77	11.7	650		8	Zo + Clz overgrowths

gated on **b** and flattened on (100). At 650°C and 6.5 kbar the average zoisite was 40 μm long while the average clinozoisite was 10 μm long, but some crystals greater than 100 μm could always be found for either material. In going from iron-free to iron-rich compositions, the major product shifted from Zo to Zo + Clz to Clz. However, the more iron-rich compositions yielded inhomogeneous crystals as evidenced by distinct variations in the interference colors. In addition, most synthesis runs contained an estimated 1 to 3% total of other phases such as silica glass, anorthite, garnet or magnetite.

The inhomogeneity of the synthesized starting materials precluded the use of standard, bulk compositional techniques for the phase equilibrium determination. However,

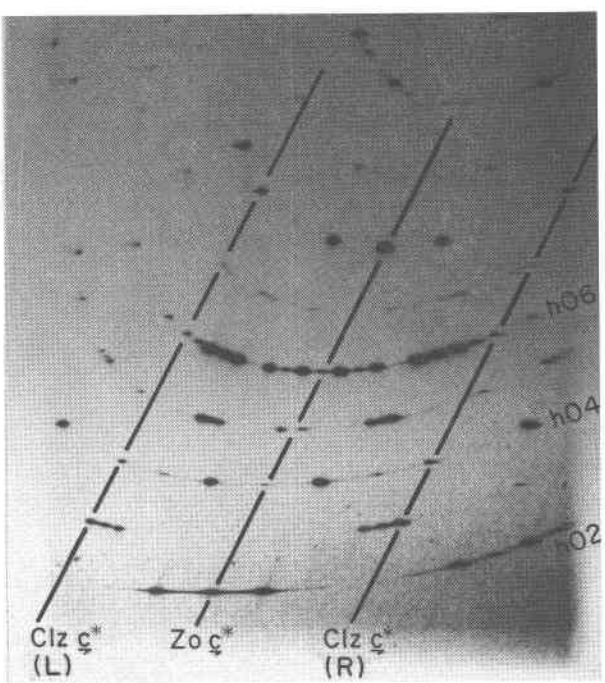

Fig. 1. Zero-level Weissenberg photograph (rotated about **b**) of an epitaxial zoisite-clinozoisite crystal. **c*** axes for zoisite and the clinozoisite twins (L,R) are shown. All have the same (*h*0*l*) layers, showing **c** to be in common.

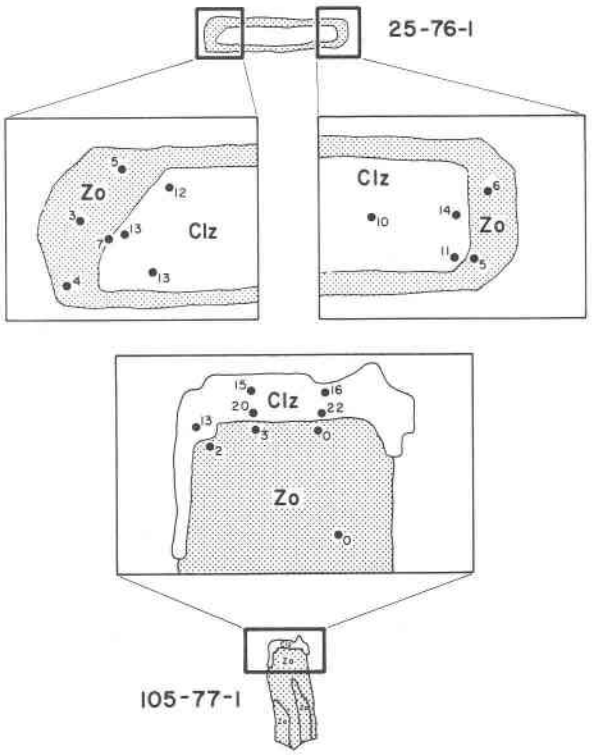

Fig. 2. Schematic diagram of epitaxial overgrowths showing compositions (in mole% Ps) determined by electron microprobe analysis: (a) a zoisite overgrowth from Run #25-76 (260 μm long, 35 μm wide); (b) a clinozoisite overgrowth from Run #105-77 (220 μm long, 110 μm wide).

it was observed that a high-iron run yielded clinozoisite crystals overgrown by zoisite (Fig. 2a), apparently due to a loss of iron to the platinum capsule. Weissenberg photographs taken with crystals rotated about their elongated direction confirmed this to be the **b** axis for both phases and that they were epitaxially related with **c** also being in common (see Fig. 1). In addition, the clinozoisite was twinned on (100). Both the crystal habit and the epitaxial relations are easily rationalized in terms of the crystal structures of these minerals (cf. Dollase, 1968). Strens (1965) reported naturally occurring overgrowths of zoisite on clinozoisite that bore the same epitaxial relation. Such overgrowths were easily distinguished under crossed-nicols since the bladed crystals naturally lie on the (100) face and show the clinozoisite core to be anomalous blue while the zoisite overgrowths are anomalous yellow. (The distinction between normal and anomalous interference colors is easily made using a Berek compensator; see Bloss, 1961, p. 144.)

Overgrowths of clinozoiste were found when iron-free zoisite seeds were placed in a high-iron bulk composition (see Table 1 and Fig. 2b). Examination of these overgrowths by X-ray and optical methods confirmed their having identical epitaxial relations to the previously described crystals.

Several of the overgrown crystals with either zoisite or clinozoisite as the overgrowth phase on clinozoisite or zoisite, respectively, were analyzed with the electron microprobe. The crystals were mounted on the enlarged (100) faces and polished until the crystal had been effectively sectioned in half; a Berek compensator was used to gauge the amount of material removed during polishing by examination of changes in retardation. Typical microprobe results for crystals synthesized at approximately 650°C and 6.5 kbar are indicated in Table 2 and Figure 2. Crystal 25-76-1 (Fig. 2a) shows an iron-rich clinozoisite core with a zoisite rim that is markedly less iron-rich. Figure 2b shows crystal 105-76-1, grown with an iron-free zoisite seed and having a clinozoisite overgrowth. This particular crystal shows the growth of iron-containing zoisite (to 3.2% Ps) before the clinozoisite could nucleate and grow. Because the anomalous interference colors could be monitored during probe analysis, there was no uncertainty in locating the phase boundary in these overgrowths and the discontinuity in iron content is genuine.

Discussion

What conclusions can be made from the observed epitaxial overgrowths and composition gap between the two phases? First, although the structures of zoisite and clinozoisite are similar, they are not identical. It is only possible for an equilibrium overgrowth to nucleate and grow when there is a finite saving in free energy by so doing. There is only one source for such a decrease in free energy: The overgrowth phase must have a lower molar free energy than the original phase of the same composition. In other words, if a clinozoisite or composition X epitaxially overgrows a zoisite, that clinozoisite must be more stable than zoisite of composition X. This relationship holds whether or not the equilibrium is stable. If the equilibrium is metastable, some assemblage other than clinozoisite of composition X will have a still lower Gibbs free energy.

This being the case, how is the composition gap at the epitaxial phase boundary related to the coexisting composition at equilibrium? Consider the schematic Gibbs free energy-composition diagram in Figure 3. As drawn, the figure shows zoisite to be the stable phase at low iron contents while clinozoisite is the stable phase at high iron contents; this agrees with our experimental observations, those of Jenkins et al. (1983), and with observations on natural materials (Enami and Banno, 1980). Compositions X1 and X3, defined by the points of common tangency (N and M), correspond to the equilibrium zoisite–clinozoisite pair. If we consider the situation where clinozoisite is the original phase, then the composition of a zoisite overgrowth would have to lie to the left of X2, the crossover point for the free energy curves. Only in this region is zoisite of lower molar free energy than a clinozoisite of identical composition. However, there is no *a priori* constraint that the zoisite lie at composition X1, the equilibrium value. The epitaxial overgrowth of zoisite on clinozoisite is expected to be an irreversible process under the conditions of these experiments and hence need not observe reversible equilibrium constraints. Furthermore, we would not expect solid state diffusion to equilibrate the coexisting compositions on a laboratory scale if natural processes leave epidote minerals compositionally zoned after much longer geologic times. Hence, we conclude that the observed compositional gap need not correspond to the equilibrium gap, but must only overlap with it. However, because of the nucleation energy necessary to grow a new phase, it is probable that the initial nucleation was at a composition where there was a significant difference in free energy between the two phases. This suggests, but clearly does not require, that the true equilibrium bracket would probably lie within our experimental bracket, not outside of it.

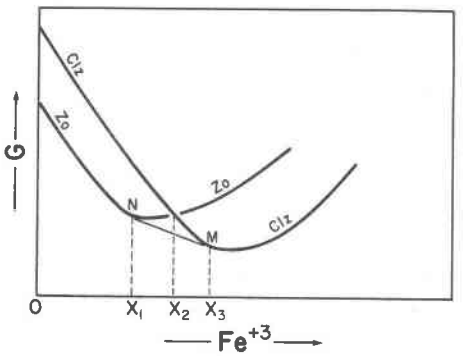

Fig. 3. Schematic Gibbs energy–composition diagram for the zoisite–clinozoisite compositional gap.

Table 2. Microprobe compositions across epitaxial phase boundary

	Clz Comp. (mole % Ps)	Zo Comp. (mole % Ps)	Crystal No.
Zoisite Overgrowth	11	5	25-76-1
	13	7*	
	8	6	25-76-2
	8	6	
Clinozoisite Overgrowth	22	0	105-77-1
	20	3	
	19	0	106-77-1
	16*	0	

*Microprobe composition taken extremely close to phase boundary and the analytical volume may have extended across that boundary.

Proceeding with that reasoning, the transition loop can be evaluated in terms of our experiments. Considering the data of Table 2, we can safely conclude that $G_{Zo} < G_{Clz}$ for $X_{Fe} \leq 6$ mole% pistacite, and $G_{Clz} < G_{Zo}$ for $X_{Fe} \geq 19$ mole% pistacite for the experimental conditions $T = 650°C$, $P = 6.5$ kbar, and an oxygen fugacity fixed at approximately the NNO buffer. Both compositional limits are those of the overgrowth phase determined near the phase boundary. There is some uncertainty about the reli-

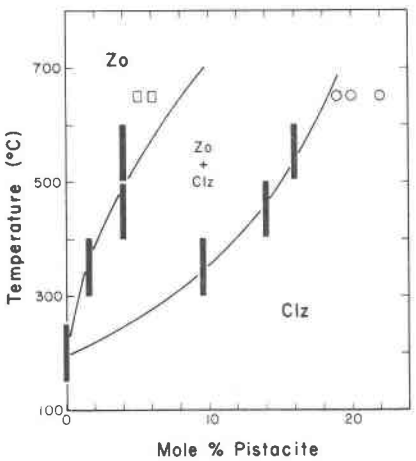

Fig. 4. Approximate zoisite–clinozoisite transition loop constructed using T–X data on coexisting, natural pairs (see text). Open squares and circles represent experimental data from Table 2 that define conditions where $G_{Zo} < G_{Clz}$ and $G_{Clz} < G_{Zo}$, respectively.

ability of the 7 mole% Ps (zoisite) and the 16 mole% Ps (clinozoisite) compositions in Table 2 because the microprobe beam was positioned extremely close to the phase boundary in both instances. These values are therefore not used in deducing the relative stability values (although examination of the arguments leading to Figure 4 shows that they are not unreasonable). It is interesting to compare these data with the compositions of naturally coexisting zoisite–clinozoisite pairs determined by Enami and Banno (1980) and by Tanner (1976), and with the iron-free ortho-clino transition temperature estimated by Jenkins et al. (1983). Following these authors, rough temperature intervals can be assigned to the sets of coexisting compositions so as to allow an approximate temperature-composition phase diagram to be constructed. For the compositions reported by Tanner from rocks in the kyanite–staurolite zone adjacent to the lowest sillimanite zone (4 and 16 mole% Ps), a temperature range of 500–600°C is used. For the greenschist facies pair of Enami and Banno (1.5 and 9.5 mole% Ps) a range of 300–400°C is used, while their upper epidote–amphibolite facies pair (4 to 14 mole% Ps) is assigned a temperature range of 400–500°C. When these data are combined with the iron-free transition temperature of 200°C ($\pm$50°C?, Jenkins et al., 1983), the phase diagram can be drawn (Fig. 4). Differences in pressure have been neglected because the molar volumes of the two phases are nearly identical (Dollase, 1968; Enami and Banno, 1980). In Figure 4 squares represent our compositions where $G_{Zo} < G_{Clz}$, while circles are used to represent our composition where $G_{Clz} < G_{Zo}$ (data from Table 2). To be sure our experimental data are limited, but they agree well with the boundaries estimated from the natural compositions, and tend to lie outside the estimated transition loop compositions.

In spite of the interesting results that have been obtained from crystal overgrowths, these few data do not directly yield experimental values for the equilibrium compositions. What is of interest, however, is that it is technically feasible and desirable to examine single crystals from an experimental run as opposed to the entire batch. With some modifications we feel that the experimental procedures described here could be employed to determine equilibrium pair compositions. First of all, starting materials should be crystalline phases rather than oxide mixes. By carefully varying the compositions and amounts of seeds and run matrix, and by monitoring the zoning and overgrowths that result, it should be possible to define the equilibrium compositions more precisely and to demonstrate reversibility. Such experiments will be even more time consuming than the ones presented here. However, the development of a useful geothermometer in low- to medium-grade basic and calcareous rocks is sufficient justification for such an effort.

References

Ackermand, D. and Raase, P. (1973) Coexisting zoisite and clinozoisite in biotite schists from the Hohe Tauern, Austria. Contributions to Mineralogy and Petrology, 42, 333–341.

Bloss, F. D. (1961) An Introduction to the Methods of Optical Crystallography. Holt, Rinehart and Winston, New York.

Dollase, W. A. (1968) Refinement and comparison of the structures of zoisite and clinozoisite. American Mineralogist, 53, 1882–1898.

Enami, M. and Banno, S. (1980) Zoisite–clinozoisite relations in low- to medium-grade high-pressure metamorphic rocks and their implications. Mineralogical Magazine, 43, 1005–1013.

Goldsmith, J. R. (1981) The join $CaAl_2Si_2O_8$–H_2O (anorthite–water) at elevated pressures and temperatures. American Mineralogist, 66, 1183–1188.

Holdaway, M. J. (1972) Thermal stability of Al–Fe epidote as a function of f_{O_2} and Fe content. Contributions to Mineralogy and Petrology, 37, 307–340.

Jenkins, D. M., Newton, R. C. and Goldsmith, J. R. (1983) Fe-free clinozoisite stability relative to zoisite. Nature, 304, 622–623.

Liou, J. G. (1973) Synthesis and stability relations of epidote, $Ca_2Al_2FeSi_3O_{12}(OH)$. Journal of Petrology, 14, 381–413.

Newton, R. C. (1965) The thermal stability of zoisite. Journal of Geology 73, 431–441.

Newton, R. C. (1966) Some calc-silicate equilibrium relations. American Journal of Science, 264, 204–222.

Rodgers, A. F. (1924) Clinozoisite from lower California. American Mineralogist, 9, 221–224.

Springer, G. (1976) Correction procedures in electron-probe analysis. In D. G. W. Smith, Ed., M.A.C. Short Course Notes in Microprobe Techniques, p. 45–62. Mineralogical Association of Canada, Edmonton.

Strens, R. G. J. (1965) Stability and relations of the Al–Fe epidotes. Mineralogical Magazine, 35, 464–475.

Tanner, P. W. G. (1976) Progressive regional metamorphism of thin calcareous bands from the Moinian rocks of N.W. Scotland. Journal of Petrology, 17, 100–134.

Manuscript received, March 8, 1984;
accepted for publication, October 16, 1984.